2023

Investigating the Effects of Immune Checkpoint Inhibition and Combined Treatment with Evofosfamide on the Tumor Microenvironment Through Hypoxia Imaging

Kaytlyn Carter McNeal
University Of Alabama At Birmingham

INVESTIGATING THE EFFECTS OF IMMUNE CHECKPOINT INHIBITION AND COMBINED TREATMENT WITH EVOFOSFAMIDE ON THE TUMOR MICROENVIRONMENT THROUGH HYPOXIA IMAGING

by

KAYTLYN CARTER MCNEAL

BENJAMIN M. LARIMER, COMMITTEE CHAIR
SUZANNE E. LAPI
ANNA G. SORACE

A THESIS

Submitted to the graduate faculty of The University of Alabama at Birmingham,
in partial fulfillment of the requirements for the degree of
Master of Science

BIRMINGHAM, ALABAMA

2023

INVESTIGATING THE EFFECTS OF IMMUNE CHECKPOINT INHIBITION AND COMBINED TREATMENT WITH EVOFOSFAMIDE ON THE TUMOR MICROENVIRONMENT THROUGH HYPOXIA IMAGING

KAYTLYN CARTER MCNEAL

MULTIDISCIPLINARY BIOMEDICAL SCIENCE

ABSTRACT

Colorectal cancer (CRC) is a prevalent and deadly cancer worldwide. While immunotherapy, particularly immune checkpoint inhibition, shows promise in various cancers, its efficacy in CRC and other tumor types is limited. Hypoxia, characterized by inadequate tissue oxygenation, critically drives cancer progression, promoting tumor growth, metastasis, chemotherapy resistance, and poor prognosis. Evofosfamide, a hypoxia-activating prodrug, is being evaluated in clinical trials for combined use with checkpoint blockade as a potential therapeutic strategy. This study investigates the impact of hypoxia on immune checkpoint inhibition, evofosfamide, and combination therapy, while utilizing non-invasive molecular imaging to develop analytical methods for quantifying and characterizing tumor hypoxia severity and distribution.

Hypoxia hampers the effectiveness of immunotherapy by facilitating immune escape and resistance to checkpoint inhibitors, emphasizing the importance of overcoming the immunosuppressive tumor microenvironment. Non-invasive measurement of tumor hypoxia is crucial for understanding its role and developing personalized treatment strategies. Traditional invasive methods have limitations in providing comprehensive spatial and temporal information, necessitating the development of non-invasive techniques. Molecular imaging, particularly positron

emission tomography (PET), revolutionizes oncology by enabling longitudinal cancer detection, monitoring, and prognosis. PET imaging with hypoxia-specific tracers like [^{18}F]-fluoromisonidazole (FMISO) provides quantitative and spatially resolved information on tumor hypoxia. FMISO selectively accumulates in hypoxic regions, identifying poorly oxygenated areas associated with aggressive tumor behavior and therapy resistance.

This study non-invasively quantifies tumor hypoxia in murine CRC models using molecular imaging techniques, specifically PET with FMISO, across diverse treatment groups to assess interventions' effects on tumor hypoxia. Various PET metrics, including tumor maximum FMISO uptake (tMax) and tumor average FMISO uptake (tAvg), characterize and quantify tumor hypoxia. Muscle metrics, such as muscle average FMISO uptake (mAvg) and muscle standard deviation (mSD), serve as reference values for normalization. PET histograms provide insights into the spatial distribution and heterogeneity of hypoxia within the tumor. This research enhances our understanding of the interplay between hypoxia and immune checkpoint inhibition in the tumor microenvironment, facilitating personalized treatment strategies targeting tumor hypoxia. Non-invasive quantification of tumor hypoxia using molecular imaging provides valuable information for treatment planning, predicting treatment response, and improving patient outcomes in various cancers and tumor microenvironments.

Keywords: colorectal cancer (CRC), immune checkpoint inhibition (CPI), hypoxia, positron emission tomography (PET), [^{18}F]-fluoromisonidazole (FMISO), evofosfamide (TH-302)

DEDICATION

I dedicate this thesis to my cherished family and beloved husband. Your constant prayers, love, encouragement, and unwavering support have been the foundation of my academic journey. Your belief in my abilities and sacrifices made along the way have enabled me to reach this milestone. I am profoundly grateful for your presence in my life, and this thesis is a tribute to the love, strength, and inspiration I draw from each of you. Thank you for being my pillars of support, and for standing by me every step of the way.

ACKNOWLEDGEMENTS

I would like to express my heartfelt appreciation to all those who have contributed to the successful completion of this thesis. First and foremost, I would like to extend my deepest appreciation to my advisor, Dr. Benjamin Larimer, whose guidance, expertise, and unwavering support have been invaluable throughout this research journey. Your mentorship and encouragement have played a significant role in shaping my understanding and fostering my growth as a researcher. I would also like to thank the members of my thesis committee, Dr. Anna Sorace and Dr. Suzanne Lapi, for their insightful feedback, constructive criticism, and valuable suggestions. Your expertise and scholarly input have greatly enhanced the quality of this work.

I would also like to extend my sincere gratitude to Graduate Multidisciplinary Biomedical Science at The University of Alabama at Birmingham. I am appreciative of the rigorous curriculum, interdisciplinary perspectives, and professional development opportunities offered by the program. I would like to acknowledge the Program Director, Dr. John Shacka, for his exemplary leadership, guidance, and continuous support throughout my graduate studies.

Furthermore, I would like to acknowledge the support and resources provided by The University of Alabama at Birmingham. The facilities, equipment, and funding have been instrumental in facilitating the progress of this research. I am grateful to my colleagues and fellow researchers who have provided stimulating discussions, valuable

insights, and a collaborative environment. Your camaraderie and intellectual exchange have been instrumental in shaping my research ideas and broadening my perspective. I would like to express my heartfelt gratitude to my family and friends for their unwavering support, love, and encouragement throughout this academic journey. Your belief in me and constant motivation have been a source of strength and inspiration.

Lastly, I would like to acknowledge the countless individuals who have contributed to the body of knowledge in my field through their published work, seminal studies, and groundbreaking discoveries. Their contributions have paved the way for this research and continue to inspire further exploration. In conclusion, I am grateful to all those who have played a part, directly or indirectly, in the completion of this thesis. Your contributions have been invaluable, and I am truly grateful for your support and collaboration.

TABLE OF CONTENTS

Page

LIST OF FIGURES

Figure *Page*

INTRODUCTION

^{18}F-FMISO PET IMAGING REVEALS THE ROLE OF HYPOXIA SEVERITY IN RESPONSE TO CHECKPOINT BLOCKADE AND MEASURES THE EFFECTS OF COMBINATION THERAPY WITH EVOFOSFAMIDE

LIST OF ABBREVIATIONS

^{11}C	carbon-11
^{64}Cu	copper-64
^{18}F	fluorine-18
^{18}F-FAZA	[^{18}F]-fluoroazomycin arabinoside
^{18}F-FMISO	[^{18}F]-fluoromisonidazole
^{68}Ga	gallium-68
^{89}Zr	zirconium-89
ANOVA	analysis of variance
AUC	area under the curve
Br-IPM	bromo-isophosphoramide mustard
C57BL/6	common strain of laboratory mice
CPI	checkpoint inhibitor
CRC	colorectal cancer
CT	computerized tomography
CTLA-4	cytotoxic T-lymphocyte–associated antigen 4
DMEM	Dulbecco's Modified Eagle Medium
evo only	evofosfamide only treatment
FBS	fetal bovine serum
FMISO	^{18}F-fluoromisonidazole
HIF1a	hypoxia-inducible factor 1-alpha

ID0	pre-evofosfamide treatment imaging day 0
ID5	post-evofosfamide treatment imaging day 5
IFNg	interferon gamma
IO only	immunotherapy only treatment
IO+Evo	combined immunotherapy and evofosfamide treatment
mAvg	muscle average FMISO uptake
MC38	murine colorectal cancer cells
MRI	magnetic resonance imaging
mSD	muscle standard deviation
NK	natural killer cells
PD-1	programmed cell death receptor 1
PD-L1	programmed cell death ligand 1
PET	positron emission tomography
real-time PCR	real-time polymerase chain reaction
RECIST	Response Evaluation Criteria in Solid Tumors
ROC	Receiver Operator Characteristics curve
ROI	region of interest
SD	standard deviation
SEM	standard error of the mean
SUVmean	standard uptake value mean
tAvg	tumor average FMISO uptake
TBR	tumor-to-blood ratio
TH-302	original name of evofosfamide

tMax	tumor maximum FMISO uptake
TMR	tumor-to-muscle ratio

CHAPTER 1

INTRODUCTION

Oncology

Oncology, the field of medicine dedicated to the prevention, diagnosis, and treatment of cancer, plays a pivotal role in addressing one of the most pressing global health challenges. In 2020, cancer's devastating global impact manifested through an estimated loss of 10 million lives, accounting for approximately one in six deaths, and an additional 19.3 million individuals receiving a cancer diagnosis [1]. Among the diverse array of cancers, several types stand out as major contributors to the global burden. Notably, lung, colorectal, stomach, breast, and liver cancers collectively account for nearly half of all cancer-related fatalities [2]. Given the alarming statistics, there is an urgent need to advance oncology therapeutics and explore avenues for improved interventions. Herein we will focus on and broadly discuss colon and rectal cancer which are collectively referred to as colorectal cancer.

Colorectal Cancer

Colorectal cancer (CRC) ranks as the third most prevalent cancer worldwide and stands as the second leading cause of cancer-related deaths [3]. Despite advancements in research, the incidence and mortality rates of CRC continue to rise [4]. This alarming trend can be attributed, in part, to the dysregulation of critical signaling pathways involved in CRC pathogenesis [5]. Moreover, mounting evidence suggests that hypoxia

plays a pivotal role in CRC progression by stabilizing hypoxia-inducible factor 1-alpha (HIF1a), which subsequently promotes the expression of genes involved in tumor vascularization, metastasis acceleration, chemotherapy resistance, and unfavorable prognosis [6-9]. Given the significant implications of hypoxia in CRC, there is an urgent need for effective treatments and monitoring strategies to better understand and combat this disease.

Immunotherapy

Immunotherapy, a cancer treatment approach that activates the adaptive immune system's anti-tumor response, has sustained substantial growth in its utilization in clinical trials and integration into standard-of-care treatment for malignant tumors [10, 11]. Recent advancements in the field have demonstrated the potential of immunotherapy in targeting and treating various types of cancers, leading to improved patient outcomes and long-term survival [12-14]. However, challenges such as resistance mechanisms and limited effectiveness in certain tumor types highlight the need for ongoing research to expand our understanding of immunotherapy's mechanisms, identify predictive biomarkers, and optimize treatment strategies, with the goal of improving outcomes and expanding its application to a wider range of cancer [15-18]. In this introduction, we will provide a broad overview of immune checkpoint inhibition, which is among the various forms of immunotherapy.

Immune Checkpoint Inhibition

The immune system of the human body is a sophisticated defense mechanism that protects against foreign invaders, including pathogens and abnormal cells such as cancer cells [19]. It involves the activation and coordination of various immune cells, such as T cells, B cells, and natural killer (NK) cells, which work together to recognize and eliminate these threats [20, 21]. Checkpoint inhibition (CPI) represents a paramount achievement in cancer immunotherapy over the past decade for unlocking the immune system to effectively target and combat cancer cells [22, 23]. Within the tumor microenvironment, there are immune checkpoints, which are regulatory pathways that prevent excessive immune activation and maintain immune homeostasis [24]. However, cancer cells exploit these checkpoints to evade immune surveillance and promote tumor growth [18].

Immune checkpoint inhibitors, such as programmed cell death receptor 1 (PD-1) and cytotoxic T-lymphocyte-associated antigen 4 (CTLA-4), block the inhibitory signals, thereby freeing the immune system to mount a robust and sustained attack against cancer cells [25]. This leads to the reinvigoration of anti-tumor immune responses, including the activation of cytotoxic T cells, enhanced tumor infiltration of immune cells, and increased production of pro-inflammatory cytokines [26]. By removing the brakes on the immune response, checkpoint inhibition has demonstrated remarkable clinical efficacy in a subset of patients across various cancer types, providing long-lasting responses and even complete remissions [27]. This therapeutic strategy has revolutionized the field of cancer treatment and holds great promise for improving patient outcomes. Nevertheless, while checkpoint blockade has shown durable clinical responses in a minority of patients,

the majority still do not experience any significant benefits. One of the challenges in checkpoint inhibition is overcoming the immunosuppressive tumor microenvironment, including factors like hypoxia, which can limit the effectiveness of immune response [28, 29].

Hypoxia

Hypoxia, characterized by inadequate tissue oxygenation, exerts a critical influence on numerous physiological and pathological processes, including cancer [30]. It serves as a key player in tumor development, stimulating angiogenesis, metabolic reprogramming, and genetic alterations that contribute to disease progression [30-33]. Insights into hypoxia-induced molecular pathways and their interplay with crucial cellular processes have laid the groundwork for innovative therapeutic strategies and biomarkers. While hypoxia shows promise as a biomarker, particularly in radiation therapy, its potential as a direct drug target has been limited in clinical trials [34, 35]. Current research endeavors aim to uncover novel perspectives on how hypoxia influences tumor heterogeneity, immune evasion, and therapeutic resistance, providing opportunities for the development of personalized treatment approaches that effectively target specific tumor subpopulations and enhance the efficacy of immunotherapy.

Immune Checkpoint Inhibition Hypoxia Resistance

The role of hypoxia in the context of immune checkpoint inhibition has gained significant attention as a key determinant of tumor immune responses and therapeutic outcomes [36]. Hypoxia has been implicated in promoting immune escape and resistance

to checkpoint inhibitors such as PD-1 and CTLA-4 [29]. Emerging evidence suggests that targeting hypoxia-driven signaling pathways or combining checkpoint inhibitors with hypoxia-modulating interventions holds promise for enhancing the efficacy of immunotherapy and improving patient outcomes [37]. However, despite the substantial impact of hypoxia on the tumor microenvironment, there is limited study on the non-invasive quantification of hypoxia in relation to immune checkpoint inhibition.

Quantifying Tumor Hypoxia

The non-invasive measurement of hypoxia in cancer has emerged as a crucial area of research with significant clinical implications. Traditional invasive methods for assessing tumor hypoxia, such as oxygen electrodes and biopsies, are limited in their ability to provide spatial and temporal information and are often impractical for repeated measurements [38]. Non-invasive techniques, including molecular imaging with hypoxia-specific tracers, have gained prominence due to their ability to provide quantitative and spatially resolved information on tumor hypoxia [39]. These methods enable the identification of hypoxic regions within tumors, which have been shown to play a critical role in tumor progression, treatment response, and patient outcomes [40].

Recent studies on hypoxia in cancer underscore its importance as a key microenvironmental factor that influences tumor aggressiveness, angiogenesis, immune evasion, and therapy resistance. Additionally, studies have highlighted the association between high levels of tumor hypoxia and poor clinical outcomes, reinforcing the need for accurate and non-invasive hypoxia measurements [41]. Moreover, advances in imaging technologies, such as positron emission tomography (PET) and magnetic

resonance imaging (MRI), have facilitated the development of novel hypoxia imaging agents and imaging biomarkers [42]. These tools have provided valuable insights into the spatiotemporal heterogeneity of tumor hypoxia and its dynamic changes during disease progression and treatment.

Molecular Imaging in Oncology

The potential of molecular imaging in oncology has revolutionized the detection, monitoring, and prognostication of cancer, leading to advancements in therapeutic strategies [43]. The personalized treatment landscape has been profoundly shaped by the utilization of highly specific, sensitive imaging techniques targeting a multitude of biological targets that are now applied in clinical practice. Notably, positron emission tomography (PET) has emerged as an invaluable modality for visualizing specific biomarkers that correlate with underlying phenotypes, complemented by the integration of computerized tomography (CT) to provide precise anatomical information [44-46]. The synergistic combination of these cutting-edge techniques has ushered in a new era of transformative breakthroughs in the field of oncology.

CT

CT has garnered widespread adoption as the imaging modality of choice for cancer staging in patients with advanced disease, owing to its accessibility, cost efficiency, and reproducibility [47]. A standard diagnostic CT scanner comprises an X-ray source and detector that rotate around the patient, capturing X-ray intensities that are processed by algorithms to generate cross-sectional images **(Figure 1-1)** [48, 49].

Furthermore, CT plays a pivotal role in determining tumor size, a critical metric utilized for assessing treatment response and applying response evaluation criteria, such as the widely used RECIST measurements in solid tumors [46, 50]. Integration of this anatomical metric with biomarker-specific imaging techniques like PET offers a wealth of invaluable data, enabling comprehensive assessments of tumor characteristics.

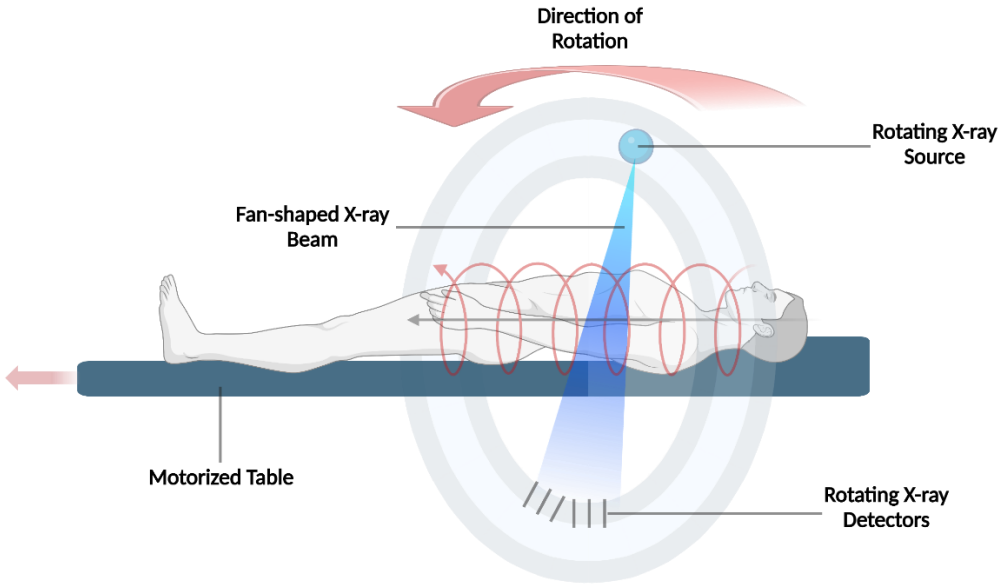

Figure 1-1. The figure depicts a clinical computerized tomography (CT) detector, where a cone or fan-shaped beam and the detectors revolve around the patient.

PET

PET, a powerful imaging modality, exploits the unique properties of energetically unstable positron-emitting radioisotopes that undergo annihilation upon interaction with neighboring electrons [45]. This annihilation event yields the simultaneous emission of two photons at precisely opposite directions (180 degrees), which are detected by a ring of scintillation detectors **(Figure 1-2)** [49, 51]. Subsequent reconstruction of this data generates images, with resolution heavily influenced by the characteristics of the

radioisotope employed [52]. Low-energy positrons emitted by isotopes like ^{18}F travel shorter distances before annihilation, resulting in higher-resolution images compared to higher-energy positrons like ^{68}Ga [53]. This energy specificity, coupled with the simultaneous detection of two photons, enables precise quantitative and spatially localized detection of isotope accumulation at all tissue depths, facilitating non-invasive measurements with exceptional precision.

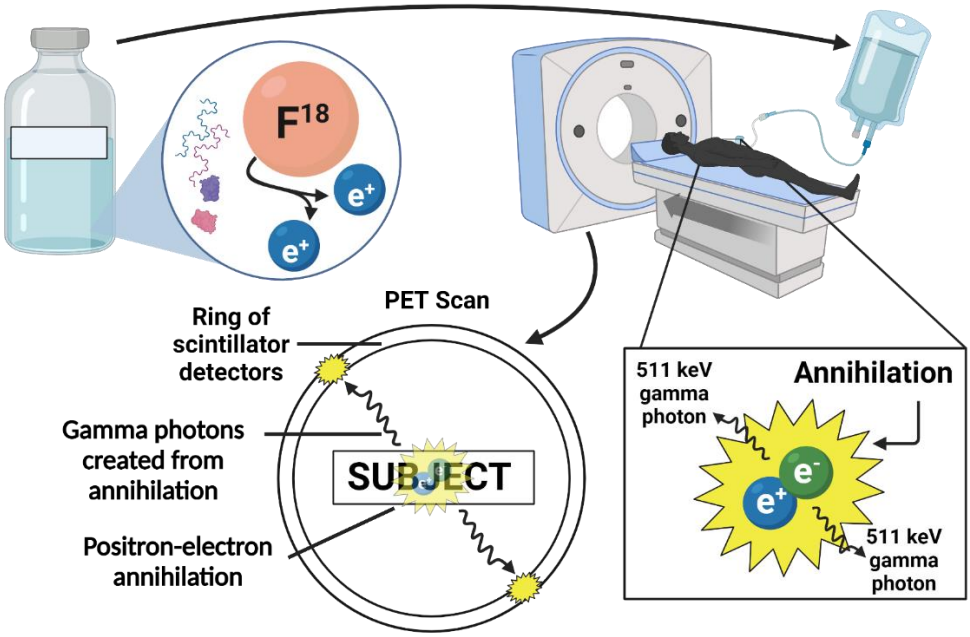

Figure 1-2. This figure represents a clinical positron emission tomography (PET) scan. An encounter between a positron and an electron leads to an annihilation event, generating two photons with an energy of 511 keV each, moving in opposite directions by 180 degrees. The simultaneous detection of the two emitted photons is accomplished through the utilization of a ring of scintillator detectors.

PET data acquisition. The acquisition and quantification of PET data are currently the subject of intensive research, encompassing technical and clinical studies aimed at deepening our understanding of the factors influencing PET measurements.

Guidelines have been proposed to standardize data variations resulting from technical and physiological factors, with the goal of improving image quality and quantitative accuracy [54]. Key data variables being investigated include region of interest (ROI) selection and background corrections. Consequently, the studies discussed in this work implement corrections for ROI delineation and background correction. The selection of ROIs plays a crucial role in PET quantification, encompassing reference regions (e.g., muscle or blood, depending on the radiotracer) as well as manually defined tumor boundaries. For tumor ROIs, normalization is conducted by dividing them by the background ROI (tumor-to-blood ratio - TBR or tumor-to-muscle ratio - TMR) for each mouse, ensuring standardized signal-to-noise ratios. Thus, all data discussed in this study adhere to accepted standards for pre-clinical studies, facilitating comparability and robust analysis.

Radiotracers. Currently, radionuclides play a crucial role in the development of radiotracers for positron emission tomography (PET) imaging, both in pre-clinical and clinical investigations [55, 56]. Prominent among the radionuclides currently being explored are carbon-11 (^{11}C), fluorine-18 (^{18}F), gallium-68 (^{68}Ga), copper-64 (^{64}Cu), and zirconium-89 (^{89}Zr). The selection of a suitable radionuclide for labeling relies on several factors, including the biological half-life of the pharmacophore and the specificities of the labeling chemistry, contributing to the successful clinical translation. Among the available radionuclides, the widely used ^{18}F (t½ = 109.7 min) stands out for PET imaging due to its combination of low positron energy (β+ avg = 0.250 MeV) and relatively short half-life. This advantageous profile has fueled extensive research on ^{18}F chemistry,

leading to the development of various radiolabeled compounds such as ^{18}F-FMISO and ^{18}F-FAZA.

[^{18}F]-fluoromisonidazole (FMISO)

FMISO, or [^{18}F]-fluoromisonidazole, is a radiotracer that has received significant attention in the field of PET imaging [57]. FMISO works based on the principle of hypoxia imaging, allowing researchers and clinicians to visualize and assess the extent of tissue hypoxia in various pathological conditions, including cancer [57]. The reduction and accumulation mechanism of FMISO in hypoxic cells is proposed to be mediated by specific enzymes, such as nitroreductases, that are upregulated under conditions of low oxygen tension **(Figure 1-3)** [49, 58]. When FMISO encounters hypoxic areas, it undergoes a reduction process in which it donates electrons to enzymes present in these cells due to the lack of oxygen as an electron acceptor. This reduction transforms FMISO into a chemically altered form that becomes trapped within the hypoxic cells. As a result, FMISO accumulates selectively in regions of inadequate oxygen supply, allowing for the visualization and quantification of hypoxic tissues using PET imaging techniques [58, 59].

FMISO has been used in preclinical and clinical studies to investigate the presence and distribution of hypoxia in tumors [60-63]. It has been found to be particularly valuable in identifying regions within tumors that are poorly oxygenated, which is associated with more aggressive tumor behavior, resistance to therapy, and poorer patient outcomes. In clinical practice, FMISO PET imaging has been employed in various cancer types, such as head and neck, lung, cervical, and glioblastoma, to guide

treatment decisions [61, 62]. It can help in identifying hypoxic regions within tumors that may be resistant to radiation therapy and may benefit from alternative treatment modalities, such as targeted therapies or hypoxia-modifying agents. Additionally, FMISO PET imaging has shown promise in predicting treatment response and prognosis, aiding in personalized treatment planning [64]. Moreover, quantitative analysis approaches, including tumor-to-background ratio calculations and voxel-based analysis, provide valuable information on the spatial distribution and heterogeneity of hypoxia within the tumor [65].

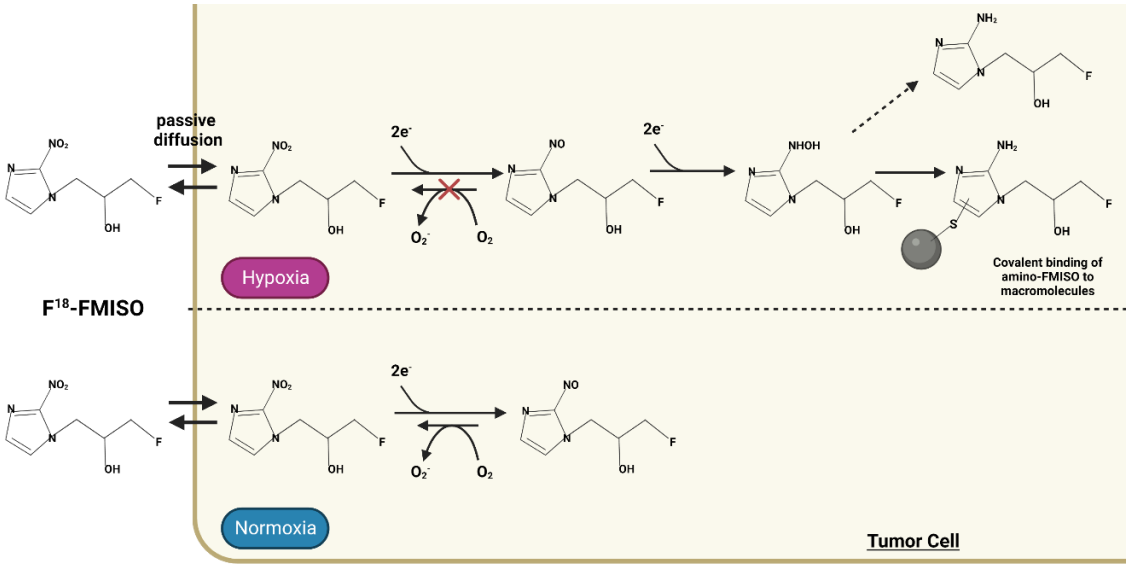

Figure 1-3. The proposed mechanism suggests that FMISO is reduced by upregulated enzymes in hypoxic cells, leading to its accumulation and retention, specifically within regions of inadequate oxygen supply.

FMISO PET Imaging Metrics

Utilization of various PET metrics play a pivotal role in quantifying and characterizing tumor hypoxia by analyzing radiotracer uptake and its association with

tumor hypoxia. One key metric is the tumor maximum FMISO uptake (tMax), which represents the highest FMISO signal intensity within the tumor volume. tMax serves as a measure of hypoxia severity and can help identify hypoxic areas within the tumor that may be associated with poor prognosis or resistance to therapy. Another important PET metric is the tumor average FMISO uptake (tAvg), which calculates the average FMISO signal intensity across the entire tumor volume. tAvg provides a quantitative measure of overall tumor hypoxia and can be used to assess treatment response and predict patient outcomes [64].

Muscle metrics, such as muscle average FMISO uptake (mAvg) and muscle standard deviation (mSD), serve as reference values for normalization and comparison purposes. Recent studies have emphasized the importance of mAvg in quantifying background FMISO uptake in non-tumor tissues [66]. By establishing a baseline FMISO uptake in the muscle, mAvg enables the differentiation between tumor-specific hypoxia and physiological variations. Additionally, mSD provides insights into the heterogeneity of FMISO distribution within the muscle, accounting for inter-individual differences and potential confounding factors.

Moreover, PET histograms have gained attention as a comprehensive tool for assessing the spatial distribution and frequency of FMISO uptake within the tumor volume [54]. Histogram analysis allows for the characterization of voxel-wise FMISO uptake patterns, providing valuable information on tumor hypoxia heterogeneity. Parameters such as the mean, median, skewness, and kurtosis derived from the histogram can provide information on hypoxia distribution and may help identify distinct subpopulations within the tumor with different hypoxic characteristics.

Integrating ^{18}F-FMISO and Immune Checkpoint Inhibitors

Tumor hypoxia has been linked to an immunosuppressive microenvironment characterized by the recruitment of regulatory T cells, myeloid-derived suppressor cells, and M2 macrophages, as well as the upregulation of immune checkpoint molecules such as PD-L1 [33]. These factors collectively contribute to impaired immune cell infiltration and function within the tumor, limiting the efficacy of CPIs [37]. The integration of FMISO PET imaging with immune checkpoint inhibition has shown promise in predicting treatment response and guiding therapeutic strategies [64]. Patients with hypoxic tumors, as identified by FMISO PET, often exhibit lower response rates and shorter progression-free survival following immune checkpoint blockade [64]. This highlights the potential of FMISO PET imaging as a non-invasive biomarker for patient stratification and selection, allowing for the identification of individuals who may benefit less from CPIs alone. Such knowledge can guide clinicians in considering alternative treatment approaches, such as combination therapies targeting both hypoxia and immune checkpoints, to overcome resistance and improve patient outcomes in hypoxic tumors.

Evofosfamide

In recent years, the use of immunostimulatory therapeutics has shown promising outcomes in a subset of patients, while a significant proportion of patients still lack effective treatment options. One potential strategy to augment immunotherapy is the incorporation of hypoxia-targeted therapeutics, which have been explored extensively, including hypoxia-activated prodrugs [67]. Among these, evofosfamide stands out as a notable example. Evofosfamide is a chemotherapy agent that selectively induces

apoptosis in hypoxic cells by reducing at the nitroimidazole prodrug site through intracellular reductases under oxygen-depleted conditions **(Figure 1-4)** [49, 68, 69]. Although evofosfamide has been evaluated in phase III clinical trials, either as a monotherapy or in combination with other chemotherapies, it did not demonstrate a statistically significant improvement in overall survival in solid tumors [70]. However, a recent phase I clinical trial investigating the combination of evofosfamide with ipilimumab, a CTLA-4 inhibitor, showed promising results, with 15 out of 18 patients achieving partial response or stable disease [71]. Nevertheless, drug-related toxicities were commonly observed in this study. These findings offer potential for enhanced treatment response and provide a strong rationale for the development of an imaging-guided personalized therapy approach to improve patient selection accuracy. Furthermore, these results highlight the prospect of utilizing evofosfamide in future diagnostic imaging applications and combination theranostics, which integrate diagnostic imaging and therapeutic interventions.

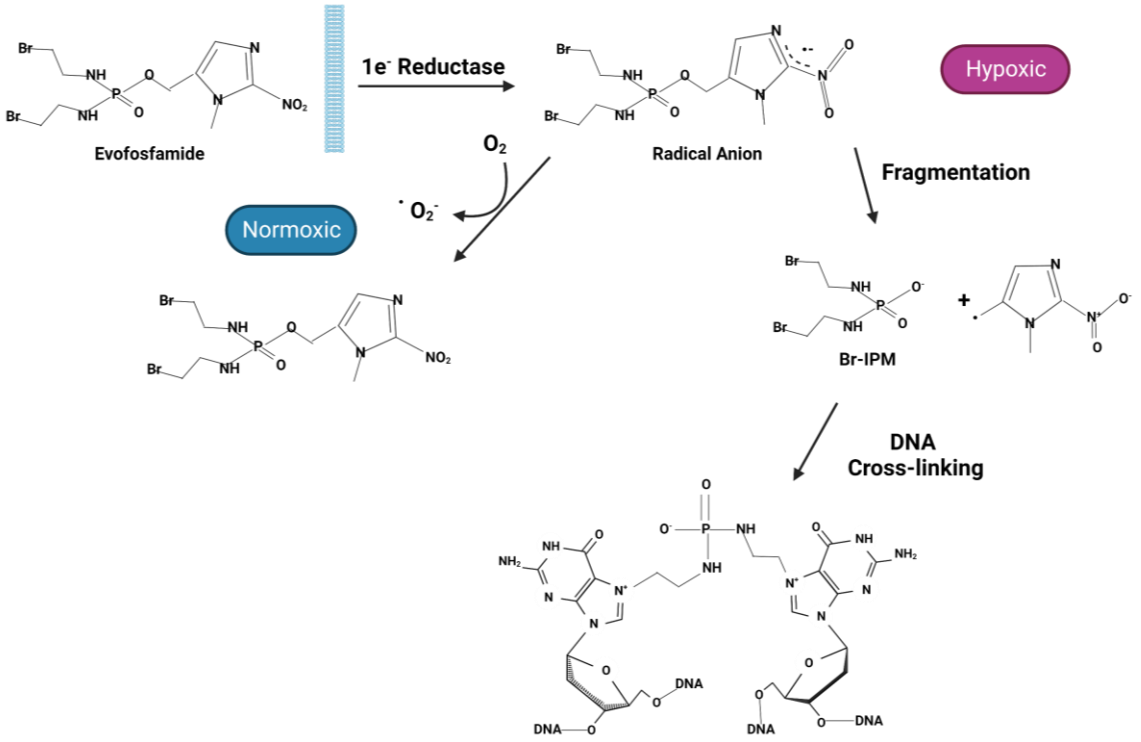

Figure 1-4. Evofosfamide (also known as TH-302) exerts its action through the following mechanism: The structure of evofosfamide consists of a nitro group. Upon entering the cell, the nitro group undergoes reduction by $1e^-$ reductases, resulting in the formation of a radical form of the drug. In normoxic conditions, this reaction is swiftly reversed, restoring the original drug. However, in hypoxic conditions, the reversal of this reaction does not occur, causing the unstable radical to fragment and generate the alkylating agent bromo-isophosphoramide mustard (Br-IPM). Br-IPM then acts by crosslinking DNA, leading to the induction of apoptosis or cell cycle arrest.

Combined Immune Checkpoint Inhibition and Evofosfamide Treatment

The utility of evofosfamide in combination with other therapeutic approaches, such as immune checkpoint inhibition, has been investigated in recent studies, showing promising results in preclinical models and early clinical trials [70, 71]. The rationale behind this combination is that evofosfamide can promote immunogenic cell death, releasing tumor antigens that can be recognized by the immune system. Preclinical

evidence suggests that evofosfamide can potentiate the antitumor immune response and enhance the efficacy of immune checkpoint inhibitors in hypoxic tumor microenvironments [64]. Hypoxia-induced immunosuppression, characterized by the upregulation of immune checkpoint molecules and recruitment of immunosuppressive cells, can limit the effectiveness of CPIs [37]. By selectively targeting hypoxic regions, evofosfamide can alleviate the immunosuppressive effects of tumor hypoxia and create a more favorable microenvironment for immune activation [64]. Studies have demonstrated that evofosfamide can sensitize hypoxic tumor cells to immune-mediated killing and enhance the infiltration and function of cytotoxic T cells within the tumor microenvironment [64, 72]. These findings suggest that the combination of evofosfamide with immune checkpoint inhibitors may offer a synergistic approach to overcome hypoxia-induced immunosuppression and improve therapeutic outcomes in cancer patients.

Project Summary

The field of clinical oncology has been revolutionized by the integration of molecular imaging, which has enhanced cancer care across various aspects of diagnosis, treatment planning, and therapeutic outcomes. This transformative impact is attributed to continuous research and development efforts in novel target-specific imaging radiotracers, enabling personalized treatment regimens and precise decision-making. In this study, we present a comprehensive exploration of the revolutionary capabilities of FMISO as a cutting-edge predictive tool for assessing treatment response pre- and post-

evofosfamide treatment. We delve into the intricate relationship between treatment response evaluations and variations in tumor hypoxia across different therapeutic modalities. Our study demonstrates that FMISO uptake provides detailed characterization of hypoxia intensity and distribution, enabling the quantification of hypoxia severity levels within individual tumor microenvironments. We show that FMISO PET output metrics can serve as predictive biomarkers for responders to immunotherapy and evofosfamide combination treatment. Furthermore, we investigate the effects of treatment over time on tumor hypoxia severity across response groups. Additionally, we discuss the implications of immunotherapy only and combined immunotherapy and evofosfamide treatment on tumor hypoxia severity. By combining diagnostic imaging with novel oncology therapies, we can gain critical insights for the development of individualized treatment approaches. The integration of molecular imaging techniques and the identification of novel therapeutic and imaging tracers play a pivotal role in optimizing patient outcomes and refining cancer management strategies. This study highlights the transformative impact of molecular imaging in clinical oncology and emphasizes the importance of ongoing research and development efforts in the pursuit of novel imaging tracers and therapeutic modalities. Through these advancements, clinicians can deliver tailored therapies, improve treatment planning, and enhance patient care in the fight against cancer.

CHAPTER 2

^{18}F-FMISO PET IMAGING REVEALS THE ROLE OF HYPOXIA SEVERITY IN RESPONSE TO CHECKPOINT BLOCKADE AND MEASURES THE EFFECTS OF COMBINATION THERAPY WITH EVOFOSFAMIDE

by

KAYTLYN C. MCNEAL, SUZANNE E. LAPI, ANNA G. SORACE, BENJAMIN M. LARIMER

In preparation for *The Journal of Nuclear Medicine*

Format adapted for thesis

Introduction

Cancer treatment has significantly changed with the advent of checkpoint inhibition, employing antibodies that target the programmed death-1 (PD-1) or cytotoxic T lymphocyte antigen-4 (CTLA-4) pathways [22, 25]. This approach has yielded durable tumor responses across various tumor types [27]. However, the presence of hypoxia within tumors has been associated with reduced efficacy of immunotherapy [18]. Hypoxia, a prevalent feature of solid tumors, arises from insufficient oxygen supply due to uncontrolled cell proliferation, altered metabolism, and abnormal blood vessel architecture [30]. Hypoxic tumor microenvironments impede immune cell access and hinder antitumor responses [28, 30, 73-75]. Despite the substantial impact of hypoxia, the non-invasive quantification of hypoxia in the context of immune checkpoint blockade has been limited.

[^{18}F]-fluoromisonidazole (FMISO), a well-established positron emission tomography (PET) tracer, provides a non-invasive method for quantifying tumor hypoxia [57]. FMISO is irreversibly trapped in hypoxic cells, enabling accurate measurement of tumor hypoxia levels [57, 76]. FMISO PET imaging has demonstrated its potential to predict response to immune checkpoint inhibitors in pre-clinical models, underscoring its role in guiding immunotherapy [64]. Recent pre-clinical findings from our group have shown that response to checkpoint blockade leads to early decreases in tumor hypoxia as measured by FMISO PET, preceding changes in tumor volume, consistent with previous studies [64]. Conversely, non-responding tumors exhibit increasing hypoxia over time, resulting in treatment failure.

To address the limitations imposed by hypoxia in immunotherapy, evofosfamide, a hypoxia-activated prodrug, has emerged as a promising solution [67, 68]. While evofosfamide monotherapy has shown limited clinical efficacy, combining it with checkpoint inhibitors has demonstrated enhanced response to immune checkpoint inhibitors in both pre-clinical and clinical settings [70, 71]. In a Phase I trial conducted by Hegde et al., combining evofosfamide with ipilimumab resulted in partial responses in 16.7% (3/18) and stable disease in 66.7% (12/18) of heavily pre-treated patients with multiple cancer types, leading to an ongoing Phase II trial [71]. Notably, all clinical studies involving evofosfamide to date have not quantified hypoxia prior to or after therapy.

Previously, our group utilized FMISO imaging to stratify checkpoint inhibitor-treated tumors before the addition of evofosfamide [64]. We observed that the addition of evofosfamide to hypoxic tumors rescued the response and increased overall survival to a level equivalent to normoxic tumors. Intriguingly, normoxic tumors treated with combination therapy also exhibited an increased response to immunotherapy. While a significant decrease in mean tumor PET signal was observed following evofosfamide treatment in the hypoxic group, no changes were observed for normoxic tumors or evofosfamide alone. These findings suggest that either the dose and timing of evofosfamide were insufficient to reduce tumor hypoxia or that standard uptake value mean (SUVmean), the conventional metric for measuring changes in hypoxia, may not be suitable. Most previous studies employing FMISO PET imaging to analyze hypoxia have primarily relied on tumor SUVmean or the ratio of tumor SUVmean to the SUVmean of a reference tissue, often muscle [64, 66]. Although these metrics have proven useful in

globally defining a tumor as hypoxic, averaging all tumor voxels diminishes the impact of heterogeneity. An alternative metric, tumor maximum FMISO uptake (tMax), can identify the maximum uptake of a tracer in a specific area and may indicate the severity of hypoxia within a tumor. However, tMax fails to provide information on hypoxia heterogeneity. Considering that evofosfamide has a substantial impact on tumor volume and overall survival, our aim was to investigate whether evofosfamide may influence regions of severe hypoxia that are not captured by the average measurement across the entire tumor.

Therefore, in this study, we conducted a comprehensive analysis employing multiple metrics, including tumor average FMISO uptake (tAvg), tMax, and histograms, to characterize and longitudinally track changes in hypoxia before and after combination therapy with evofosfamide and checkpoint blockade. Given the critical role of hypoxia in antitumor immunity and the potential of evofosfamide to rescue checkpoint blockade response, understanding the optimal metrics for assessing the effects of hypoxia on the tumor immune microenvironment will enhance the pursuit of personalized cancer treatment. In this context, FMISO PET imaging holds significant promise as a valuable tool for non-invasive quantification of tumor hypoxia. By imaging the distribution of FMISO uptake, it becomes possible to assess the spatial heterogeneity of hypoxia across the tumor.

The current study aims to leverage FMISO PET imaging to evaluate the effects of checkpoint blockade and evofosfamide therapy on tumor hypoxia severity. By employing spatial analysis techniques, such as tAvg, tMax, and histograms, we seek to characterize the heterogeneity of hypoxia within tumors and track its changes over time. This

approach will provide insights into the dynamic nature of hypoxia and its potential modulation by combination therapy, offering valuable information for predicting response to immunotherapy and gaining a deeper understanding of the mechanism of action of evofosfamide. The findings from this study have important implications for the field of cancer treatment. By elucidating the relationship between hypoxia, immunotherapy response, and the impact of evofosfamide, we can identify novel strategies to overcome the limitations imposed by hypoxia and enhance the efficacy of immunotherapeutic interventions. Moreover, the optimized use of FMISO PET imaging metrics will enable more accurate assessment and monitoring of hypoxia, facilitating the development of personalized treatment approaches tailored to the specific hypoxic characteristics of individual tumors.

Methods

Cell Culture

MC38 murine colorectal cancer cells, an immunogenic, grade III adenocarcinoma with microsatellite instability, were obtained from Kerafast. The cells were cultured in Dulbecco's Modified Eagle Medium (DMEM) supplemented with 10% fetal bovine serum (FBS), 2 mmol/L L-glutamine, and 1 mmol/L sodium pyruvate. Culturing was performed in a humidified incubator at 37°C with 5% CO_2. The cells were maintained at passage numbers below 20, and experiments were conducted using cells acquired and frozen within 1 month to preserve their phenotype. Pathogen testing, including

Mycoplasma detection via real-time polymerase chain reaction (real-time PCR) by Charles River Research Animal Diagnostic Services, confirmed the absence of contaminants. All cell lines were used within 6 months of testing.

Tumor Model

Animal procedures and housing were carried out in compliance with the guidelines of the Institutional Animal Care and Use Committee of The University of Alabama at Birmingham. C57BL/6 mice (6- to 12-week-old) from Charles River Laboratories were subcutaneously injected in the upper right shoulder with approximately 5×10^5 MC38 cells suspended in 40% Matrigel and 60% serum-free DMEM. Tumors were allowed to grow until reaching a volume of 100 mm^3 (7–10 days post-inoculation), at which point individual tumor measurements were recorded. The tumors were then allocated to groups to ensure equal distribution of tumor volumes. Treatment consisted of intraperitoneal injections of either saline or a combination therapy of 200 μg anti-PD-1 (clone RPM1–14, Bio X Cell) and 100 μg anti-CTLA-4 (clone 9H10, Bio X Cell) on days 0, 3, and 6 post-tumor inoculation. In addition, mice were treated with intraperitoneal injections of either saline or 50 mg/kg evofosfamide (TH-302 Selleckchem Catalog No. S2757) on days 6 to 10 following tumor inoculation. Tumor volume was assessed every other day to monitor changes in longitudinal tumor viability.

Radiotracer Synthesis

^{18}F-FMISO was synthesized by The University of Alabama at Birmingham's Cyclotron Facility using GE FastLab2 or Synthra RNplus synthesizers, following previously described methods [77-79]. The chemical and radiochemical purity of the final product was confirmed using high-performance liquid chromatography, and the radionuclidic purity was verified using a high-purity germanium detector. The overall non-decay-corrected yields were approximately 26%. ^{18}F-FMISO was obtained with an average radiochemical purity of >95% and a specific activity of >2,000 Ci/mmol.

^{18}F-FMISO PET Imaging

MC38 mice (N = 34) were imaged with ^{18}F-FMISO-PET on pre-evofosfamide treatment day 0 and post-evofosfamide treatment day 5. Approximately 150 μCi of ^{18}F-FMISO was injected via retro-orbital injection, and after 80 minutes, the mice were transferred for preclinical small animal PET/CT imaging using Sofie Biosciences equipment. Anesthesia was maintained with 2% isoflurane in air, and body temperature was maintained at 37°C. Static PET images were acquired for 20 minutes, and CT images were acquired for 5 minutes. The uptake of ^{18}F-FMISO in the tumor and muscle was quantified by drawing regions of interest (ROI) with CT anatomic guidance. Tumor volume, tMax, tAvg, average muscle FMISO uptake (mAvg) and muscle standard deviation (mSD) were determined from the ROI measurements in Bq/mL. Mice were monitored for an additional 15 days after the final evofosfamide treatment to assess long-term changes in tumor viability.

Histograms and Hypoxia Severity Fractions

Histogram data for each tumor ROI was calculated as a percentage of voxels per PET signal bin and plotted as group averages corrected using the standard error of the mean (SEM). The PET signal range from 0 to 475,000 Bq/mL was divided into 40 bins to capture the distribution of PET signals. To establish background control for PET signal analysis, the histogram data of each mouse tumor ROI was divided based on muscle ROI measurements. The hypoxia severity fraction was determined by standardizing the histogram data using the average (mAvg) and standard deviation (mSD) of the PET signals in the muscle ROI. The percentage of voxels per PET signal bin below mAvg represented normoxic tumors, while moderately and severely hypoxic tumors were defined by the percentage of voxels per PET signal bin ranging from mAvg to just under mAvg+2(mSD) and at mAvg+2(mSD) and above, respectively.

Statistical Analysis

All statistical analyses were conducted using GraphPad Prism Version 9 software (GraphPad Prism, RRID:SCR_002798). For assessing correlations between imaging and tissue-based analyses, paired t-tests, unpaired t-test, multiple unpaired t-tests, ANOVA, or Receiver Operator Characteristics (ROC) curves were performed. Specific comparisons were determined based on the therapeutic modality or combination of therapies, with an underlying hypothesis guiding the analyses, and therefore no adjustments for multiple comparisons were made. Correlations were considered statistically significant if the p-value for rejecting the null hypothesis of a zero slope was

less than 0.05. Assumptions underlying the tests were evaluated, and when necessary, transformations or non-parametric tests were applied. The results were reported as mean values ± standard deviation (SD) or appropriate statistical measures, ensuring the accuracy and reliability of the study.

Results

Severe Hypoxia is a Predictive Biomarker of Response to Evofosfamide Combination Treatment

The potential of [^{18}F]-fluoromisonidazole (FMISO) PET imaging to predict treatment outcomes for evofosfamide in combination with immunotherapy (IO+Evo) was investigated in mice implanted with MC38 murine colorectal cancer cells. FMISO PET imaging was utilized to monitor changes in tumor hypoxia longitudinally, with a focus on pre-evofosfamide treatment imaging day 0 (ID0), which is five days after beginning immunotherapy treatment. Tumors were stratified into responders and non-responders based on subsequent therapeutic response to evofosfamide by using the final post-evofosfamide treatment tumor volumes from day 26 of this study. The qualitative images in **Figure 1A** show visual distinctions between FMISO signal intensity in non-responders (left) and responders (right), indicating tumor hypoxia and normoxia, respectively.

Quantitative analysis of tumors demonstrated that low tMax and tAvg were predictive biomarkers for responders to immunotherapy and evofosfamide combination treatment. Specifically, the tAvg of IO+Evo responders was significantly lower than non-

responders (P=0.0127). Likewise, the tMax of IO+Evo responders was also significantly diminished (P=0.0019) when compared to non-responders **(Figure 1B, 1C)**. Receiver operating characteristic (ROC) curves were calculated to determine the predictive capabilities of these binary predictive metrics. A tMax threshold of less than 196373 Bq/mL was 100% sensitive and specific for response prediction (ROC P=0.0167, AUC=1.00). The tAvg PET signal threshold of 97926 Bq/mL trended toward being a significant predictor of response but was inferior to tMax (ROC P=0.0527, AUC=0.9048) **(Figure 1D)**. These data indicated that the presence of an area with severe hypoxia rather than the mean tumor hypoxia of an entire tumor was the most predictive of resistance to checkpoint blockade plus evofosfamide therapy.

Given the importance of individual regions of hypoxia, the role of PET signal intensity and tumor heterogeneity in response to evofosfamide combination therapy was next explored by extracting tumor histogram data for the combination therapy response group mice on imaging day 0. Histograms were used to assess the distribution of hypoxia intensity across all tumor voxels. Qualitatively, responding tumors had a higher percentage of voxels skewed toward low PET signal compared to non-responders **(Figure 1E)**. To quantify the distribution of hypoxia within a tumor, thresholds were determined based on the PET signal in reference muscle tissue. Three hypoxia severity thresholds were developed based on mean muscle uptake, with tumors below the threshold classified as normoxic, and those within one or nearly two muscle standard deviations above the mean indicating moderate hypoxia, while tumors at or beyond two standard deviations were categorized as severely hypoxic. Based on these criteria, IO+Evo responders had similar voxels that were normoxic, but significantly more

moderately hypoxic voxels and significantly lower severe (P=0.0010) hypoxic voxels compared to non-responders **(Figure 1F)**. This data supported diminished tMax as a threshold for response prediction prior to evofosfamide therapy.

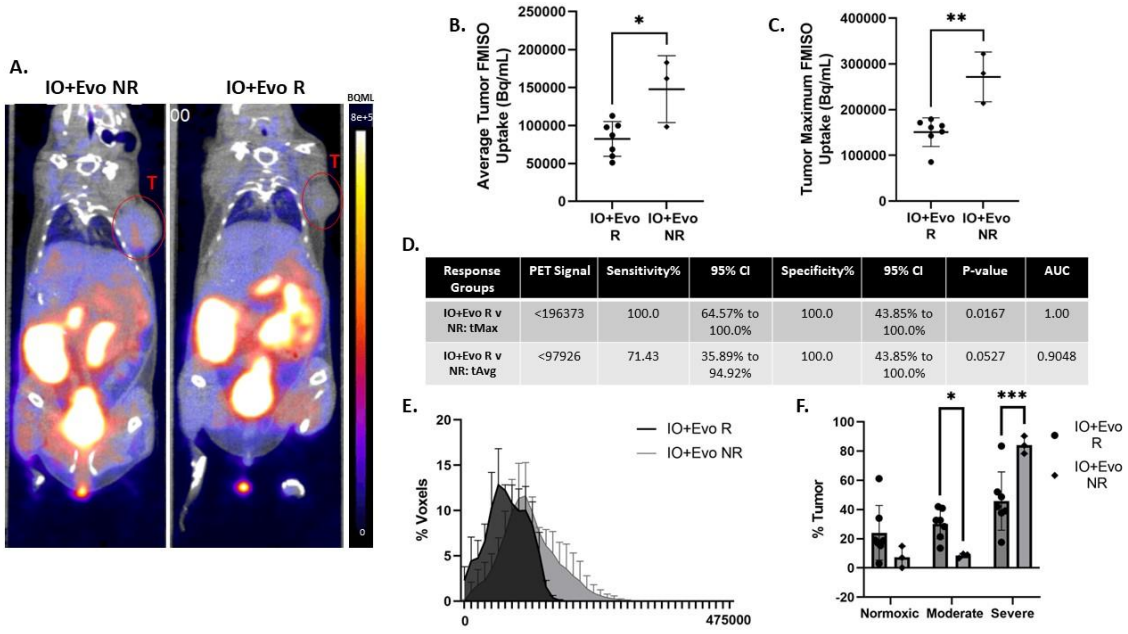

Response Groups	PET Signal	Sensitivity%	95% CI	Specificity%	95% CI	P-value	AUC
IO+Evo R v NR: tMax	<196373	100.0	64.57% to 100.0%	100.0	43.85% to 100.0%	0.0167	1.00
IO+Evo R v NR: tAvg	<97926	71.43	35.89% to 94.92%	100.0	43.85% to 100.0%	0.0527	0.9048

Figure 2-1. ***Severe Hypoxia is a Predictive Biomarker of Response to Evofosfamide Combination Treatment.*** **(A)** Representative PET/CT images of MC38 tumor-bearing mice categorized as non-responders (left) and responders (right). Tumors are highlighted by red circles and labeled as 'T.' **(B,C)** Comparative analysis of the tAvg and tMax demonstrated significant differences between IO+Evo responders and non-responders. Vertical lines indicate tumor means, and error bars represent SD. **(D)** ID0 ROC curve characteristics showing the predictive capability of tMax and tAvg for IO+Evo treatment response. **(E)** Histograms presenting the distribution and frequency of hypoxia intensity across all tumor voxels in the IO+Evo response groups. The x-axes of both histograms represent 40 PET signal bins ranging from 0 to 475,000 Bq/mL. Shaded areas indicate the mean percentage of voxels per PET signal bin, and error bars represent the standard error of the mean (SEM). **(F)** Comparison of tumor hypoxia severity thresholds. Bars represent tumor means, and error bars indicate SD. * $P < 0.05$; ** $P < 0.01$; *** $P < 0.001$.

Minimal Variation in Tumor FMISO PET Uptake Observed with Evofosfamide and Immunotherapy Treatments

We next sought to measure the changes that evofosfamide induced when combined with immunotherapy versus immunotherapy and evofosfamide alone. On post-evofosfamide treatment imaging day 5 (ID5), PET/CT scans of mice in the control, evofosfamide only (evo only), and immunotherapy only (IO only) treatment groups demonstrated similar levels of tumor FMISO PET signal **(Figure 2A)**. There were no differences in average tumor uptake or tMax for evofosfamide only treatment versus the control treatment group **(Figure 2B)**. Similarly, tumor histograms for both groups showed almost complete overlap of FMISO signal distribution **(Figure 2C)**. Additionally, there were no significant differences in either tAvg or tMax when comparing the control group to the immunotherapy group **(Figure 2D)**. Despite similar average tumor FMISO uptake, immunotherapy did result in a pronounced shift towards individual voxels with lower PET signal **(Figure 2E)**. A significant decrease in tMax (P=0.0283) of the immunotherapy group was observed when compared to the evofosfamide only group **(Figure 2F)**, suggesting distinctly opposing effects of each therapy on FMISO uptake in tumors. Likewise, histogram comparisons between the evo only and IO only groups exhibited a marked shift, with IO exhibiting a larger number of voxels with diminished FMISO uptake **(Figure 2G)**.

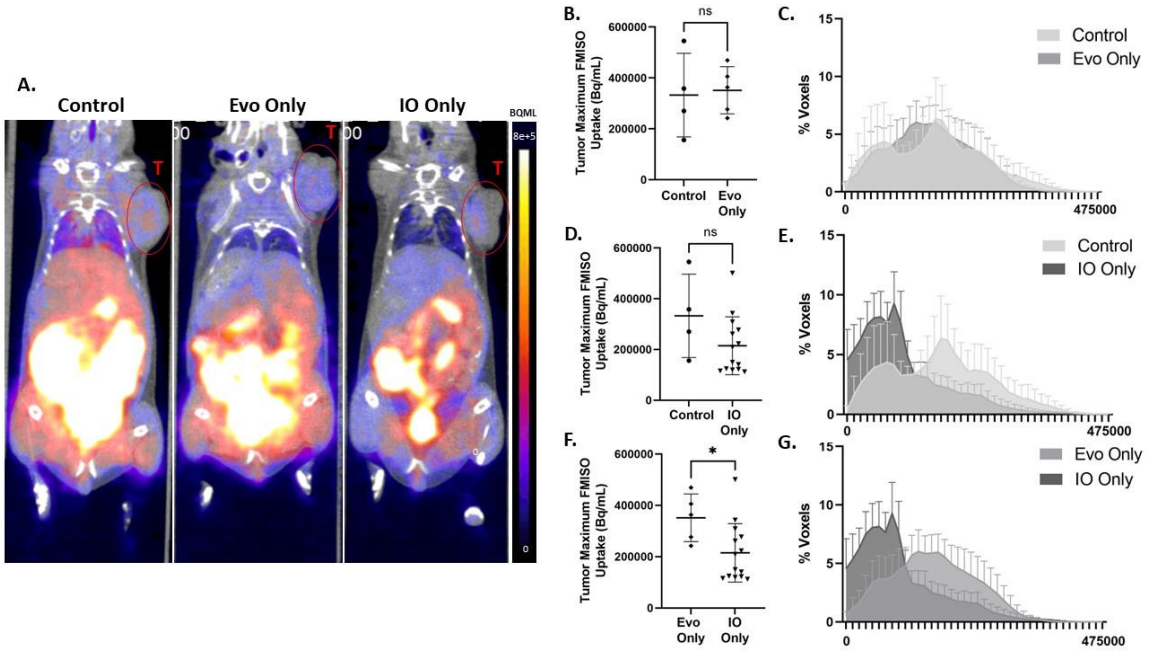

Figure 2-2. ***Minimal Variation in Tumor FMISO PET Uptake Observed with Evofosfamide and Immunotherapy Treatments*****. (A)** ID5 PET/CT scans of mice in the control, evo only, and IO only treatment groups. Red circles are drawn around tumors and labeled as 'T.' **(B)** Comparison of group tMax and histograms values across treatment control and evo only groups **(B,C)**, control and IO only **(D,E)** and evo only versus IO only groups **(F,G)**. For tMax comparisons, the center horizontal lines represent the mean of tumors and error bars measure SD. The x-axes of both histograms represent 40 PET signal bins divided over a range of 0 to 475,000 Bq/mL. Shaded areas represent the mean percentage of voxels per PET signal bin and the error bars represent the SEM.

Immunotherapy but Not Evofosfamide Reduces Tumor Hypoxia

To evaluate the addition of evofosfamide to immunotherapy, the tumor FMISO PET signal uptake intensity was qualitatively analyzed on imaging day 5. FMISO uptake exhibited a progressive decrease in signal intensity across treatment groups with the highest uptake in the control group and the lowest in the combination therapy group **(Figure 3A)**. A comparison of tMax across all treatment groups revealed a significant

decrease in tumor FMISO signal in the IO+Evo group when compared to the evofosfamide only group (P=0.0058), while no significant difference was observed between the IO+Evo and immunotherapy only groups **(Figure 3B, 3C)**. These data indicated that the addition of evofosfamide to checkpoint blockade did not have an effect on the tMax. This was despite an increased effectiveness of combination treatment in comparison to immunotherapy alone (P=0.0295) and the control group (P=0.0139), suggesting the effects of evofosfamide were not due to changes in hypoxia **(Figure 3D)**.

Figure 3E depicts each imaging day 5 histogram side-by-side based on treatment group. Histogram analysis of FMISO uptake intensity exhibited a higher concentration of voxels at low PET signals in the IO+Evo group compared to the evo only group, which shows a more even distribution across a large range of PET signals **(Figure 3F)**. In contrast, the IO only and IO+Evo groups exhibited a similar distribution of FMISO uptake intensity and show considerable overlap **(Figure 3G)**. Hypoxia severity analysis revealed increases in normoxia and decreases in severe hypoxia in the immunotherapy treated groups, but no significant differences in moderate hypoxia between treatment groups **(Figure 3H)**. Despite significant differences in means between the groups, the bifurcation of individual tumors limited significance. Given that within each treatment group there was a mix of responders and non-responders, we next sought to analyze treatment groups by response status.

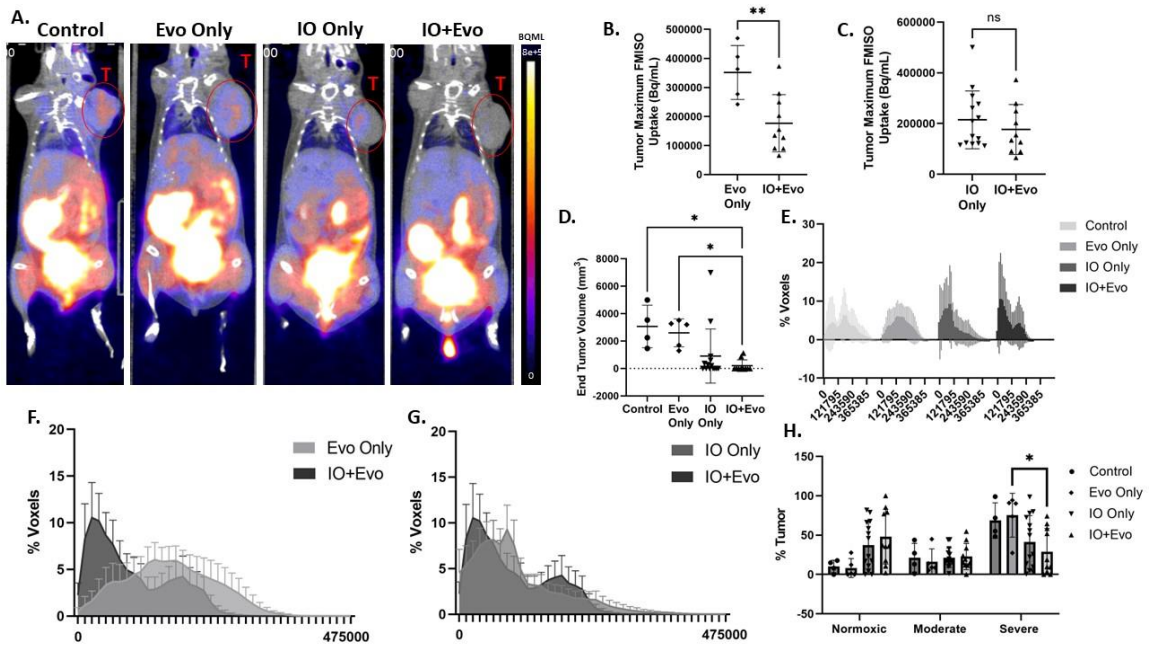

Figure 2-3. ***Immunotherapy but Not Evofosfamide Reduces Tumor Hypoxia.*** **(A)** Qualitative analysis of PET/CT images on ID5 reveals a progressive decrease in signal intensity across treatment groups. Red circles are drawn around tumors and labeled as 'T.' Comparison of group tMax values for **(B)** IO+Evo versus evo only treatment groups and **(C)** IO only versus IO+Evo treatment. Center horizontal lines represent tumor means, and error bars indicate SD. **(D)** Comparison of end tumor volume (mm^3) on day 26 of the study for all treatment groups. Center horizontal lines represent tumor means, and error bars indicate SD. **(E)** Side-by-side depiction of ID5 histograms based on treatment group. The x-axes of all histograms represent 40 PET signal bins ranging from 0 to 475,000 Bq/mL (modified for clarity). Shaded areas represent the mean percentage of voxels per PET signal bin, and error bars represent the SEM. Comparison of histograms from **(F)** IO+Evo versus Evo only and **(G)** IO+Evo versus IO only. The x-axes of both histograms represent 40 PET signal bins ranging from 0 to 475,000 Bq/mL. Shaded areas represent the mean percentage of voxels per PET signal bin, and error bars represent the SEM. **(H)** Hypoxia severity analysis between all treatment groups. Bars represent tumor means, and error bars indicate SD.

Comparing Tumor Hypoxia Severity and Distribution Between Responders and Non-responders

As only the immunotherapy and evofosfamide plus immunotherapy groups elicited responding tumors, these groups were stratified based on response for comparison. Similar to the pre-treatment predictive metric, the tMax of IO only responders were significantly lower than non-responders **(Figure 4A)**. The histogram analysis showed that the IO only responder group had a higher concentration of voxels at low PET signals, while the non-responders had a more even distribution of signal across a wider range of PET signals **(Figure 4B)**. Similar changes were seen in the combination therapy response groups, with a significant decrease in tMax for responders compared to non-responders **(Figure 4C)**. The histogram analysis was marked by a large concentration of tumor voxels with low PET signal **(Figure 4D)**. In fact, there was significant overlap and little variation in FMISO signal intensity distribution when analyzing the histograms for immunotherapy and combination therapy responders **(Figure 4E)**. Quantitatively, responders demonstrated significant decreases in severe hypoxia for both immunotherapy only (P=0.0030) and combination therapy responders (P=0.0181) when compared to their respective non-responders **(Figure 4F)**. Interestingly, reduction in severe hypoxia was accompanied by an increase in normoxia, with moderate hypoxia remaining unchanged.

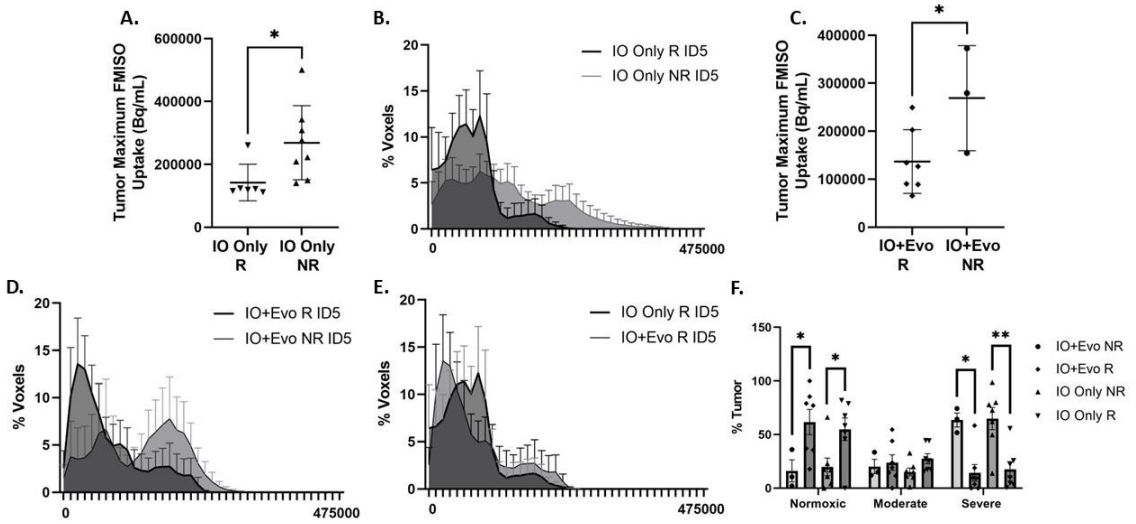

Figure 2-4. ***Comparing Tumor Hypoxia Severity and Distribution Between Responders and Non-responders.*** **(A)** Comparison of tMax between IO only responders and non-responders. Center horizontal lines represent tumor means, and error bars indicate SD. **(B)** Histogram of IO only responders versus non-responders. The x-axes of all histograms represent 40 PET signal bins ranging from 0 to 475,000 Bq/mL. Shaded areas represent the mean percentage of voxels per PET signal bin, and error bars represent the SEM. **(C)** Comparison of tMax between IO+Evo responders and non-responders. **(D)** Histogram analysis IO+Evo responders versus non-responders. **(E)** Histogram comparison of IO only and IO+Evo responders. **(F)** Hypoxia severity comparisons for responders and non-responders of both IO only and IO+Evo treatment groups. Bars represent tumor means, and error bars indicate SD.

Temporal Analysis of Hypoxia Distribution in Responding and Non-Responding Tumors

Given the significant difference in hypoxia severity and distribution between responders and non-responders from the same treatment group, we next sought to understand how these changes occurred over time. Tumor histogram analysis for immunotherapy responders over time showed direct overlap of FMISO uptake which was concentrated at low PET signals **(Figure 5A)**. In immunotherapy responders, severe hypoxia decreased and normoxia increased over time, with little variation in moderate

hypoxia **(Figure 5B)**. These data further support that effective immunotherapy acts to decrease hypoxia. In contrast, the immunotherapy only non-responders histograms revealed a significant increase in the number of voxels with high FMISO PET signal, indicating an increasingly hypoxic tumor **(Figure 5C)**. In these non-responders, there was a small decrease in normoxia and moderate hypoxia, with a slight increase in severe hypoxia in the tumors of these mice **(Figure 5D)**.

Analysis of the histograms for combination therapy responders over time had considerable overlap, but the ID5 distribution peaked at lower PET signals and extended into higher PET signals than on ID0 **(Figure 5E)**. When investigating the changes to hypoxia severity over time in the combination therapy responders, there was an increase in normoxia and decrease in severe hypoxia over time, as well as a slight decrease in moderate hypoxia **(Figure 5F)**. In contrast to responders, the histograms for the combination therapy non-responders showed a broad peak at low PET signals on ID0 which extended to a low broad peak at higher PET signals on ID5 **(Figure 5G)**. Interestingly, the tumor hypoxia severity for the IO+Evo non-responders presented a decrease in severe hypoxia and slight increases in normoxia and moderate hypoxia **(Figure 5H)**.

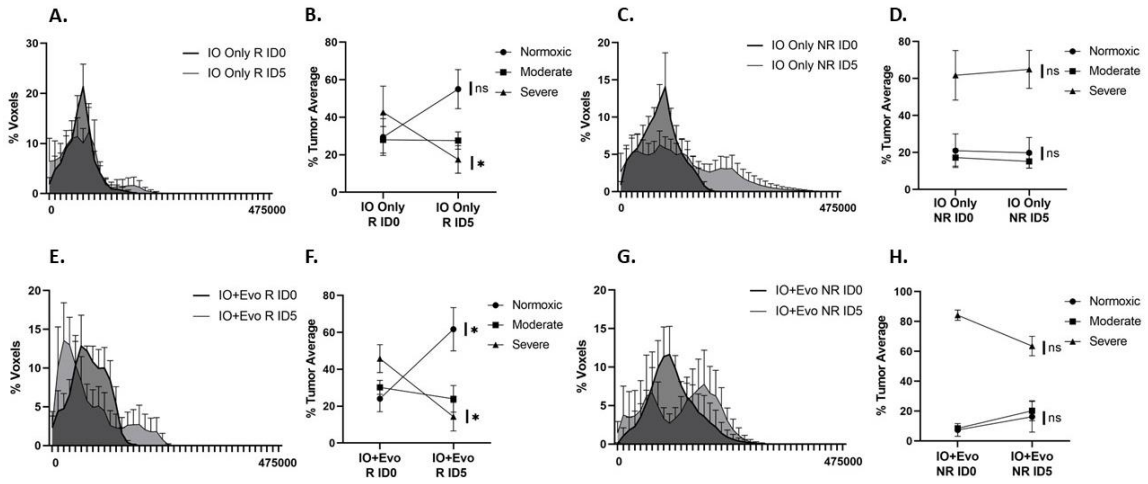

Figure 2-5. ***Temporal Analysis of Hypoxia Distribution in Responding and Non-Responding Tumors.*** Comparison of histogram analysis of hypoxia distribution and changes in the hypoxia severity distribution for IO only responders **(A,B)**, IO Only non-responders **(C,D)**, IO +Evo responders **(E,F)** and IO+Evo non-responders **(G,H)**. The x-axes of both histograms represent 40 PET signal bins ranging from 0 to 475,000 Bq/mL. Shaded areas represent the mean percentage of voxels per PET signal bin, and error bars indicate the SEM. Symbols represent grouped means per treatment, error bars indicate the SEM, and P-values were derived from paired t-test analyses.

Discussion

Our study demonstrates the efficacy of FMISO PET imaging as a non-invasive and early predictive tool for combination therapy involving immune checkpoint inhibitors and evofosfamide. By assessing tumor hypoxia using FMISO PET imaging, we identified lower tMax and tAvg measurements as strong indicators of a positive response to combination treatment. Notably, tMax emerged as the superior predictive biomarker based on ROC analysis. The fact that tMax is the strongest indicator of response suggests

that localized areas of severe hypoxia may have a global effect on tumors. This observation raises the possibility that there is a threshold of hypoxia beyond which immunotherapy and evofosfamide cannot be successful. Future studies should explore this threshold and its implications for treatment outcomes.

Through our investigation of hypoxia severity, we found that checkpoint blockade, with or without evofosfamide, effectively reduced the fraction of tumors exhibiting severe hypoxia while not affecting moderate hypoxia. This highlights the potential of immune therapies in mitigating severe hypoxia within the tumor microenvironment. Building upon previous studies, our research sheds light on the unique correlation between hypoxia and immunotherapy. Liu et al. previously demonstrated that type I immune responses have the potential to induce vascular normalization and improved blood oxygenation through interferon gamma (IFNg) signaling, which can contribute to the reduction of tumor hypoxia [80]. Our findings are consistent with their work, supporting the use of checkpoint blockade prior to additional therapies such as radiation, in order to reduce hypoxia and improve response [81].

Additionally, we observed that evofosfamide, despite its hypoxia-selective design, did not significantly reduce tumor hypoxia at the given dose and schedule. This may suggest that the dose and timing of evofosfamide in our study were not optimal for inducing hypoxia reduction. Further investigations are warranted to explore the dose-response relationship and optimal treatment schedule of evofosfamide in combination with immune checkpoint inhibitors to enhance its hypoxia-reducing potential. Importantly, even though evofosfamide did not directly reduce hypoxia, it improved the response to immunotherapy, suggesting other immune-stimulating mechanisms at play.

Moreover, our findings highlight the impact of immune checkpoint inhibitors in reducing severe hypoxia within the tumor microenvironment. The incorporation of evofosfamide further enhances the efficacy of immunotherapy, despite the lack of hypoxia reduction observed. These insights have immediate implications for translation into clinical trials, facilitating improved prediction and efficacy of combination therapy in cancer treatment.

The integration of FMISO PET imaging into clinical practice holds promise for personalized medicine, allowing clinicians to tailor treatment strategies based on the individual hypoxia profile of patients. Further research is needed to unravel the precise mechanisms underlying the potentiation of immunotherapy by evofosfamide and to optimize the dose and schedule of evofosfamide administration. Moreover, investigations into the threshold of hypoxia beyond which immunotherapy and evofosfamide cannot be successful are warranted, as this information could guide treatment decisions and enhance treatment outcomes.

CHAPTER 3

CONCLUSIONS AND FUTURE DIRECTIONS

In this study, we investigated the impact of tumor hypoxia on the efficacy of immune checkpoint blockade and the potential of evofosfamide, a hypoxia-activated prodrug, to enhance immunotherapy response. We utilized FMISO PET imaging to non-invasively quantify tumor hypoxia and employed multiple metrics, including tAvg, tMax, mAvg, mSD, and histograms, to assess hypoxia severity and heterogeneity. Our findings demonstrate that severe hypoxia is a predictive biomarker of response to evofosfamide combination treatment, with low tMax and tAvg PET signals being significantly associated with responders. The analysis of tumor histograms further revealed that responders exhibited a higher percentage of voxels with low PET signals, indicative of reduced hypoxia. Moreover, our study elucidated the variation in tumor FMISO PET uptake following evofosfamide and immunotherapy treatments, suggesting that immunotherapy alone, and especially in combination with evofosfamide, significantly alter tumor hypoxia levels by reducing severe hypoxia. These results emphasize the importance of combination therapy approaches to modulate the tumor microenvironment and overcome hypoxia-associated treatment resistance.

The implications of this research extend beyond the specific combination of evofosfamide and immunotherapy. By utilizing FMISO PET imaging and exploring different hypoxia metrics, we gain a better understanding of the dynamic nature of tumor hypoxia and its impact on immunotherapy response. This knowledge can guide the development of personalized treatment strategies that consider the hypoxic characteristics of individual tumors. Additionally, our findings highlight the potential of FMISO PET imaging as a valuable tool for accurately assessing and monitoring tumor hypoxia, which can aid in patient selection, treatment monitoring, and the design of clinical trials.

Building upon the insights gained from this study, future research directions can explore the integration of advanced MRI techniques to measure perfusion, diffusion, and cellularity, which may provide complementary information about tumor oxygenation status. Such integration of multiple imaging modalities could enhance the accuracy and comprehensive assessment of tumor hypoxia, potentially leading to improved prediction of treatment response and patient outcomes. Additionally, conducting clinical trials to validate the findings from preclinical models would be an important next step. By incorporating imaging techniques like FMISO PET, the trials can stratify patients based on their hypoxia levels, allowing for a more precise evaluation of the therapeutic response in hypoxic tumors. Assessing the predictive value of FMISO PET imaging and the identified hypoxia metrics in human cancer patients receiving evofosfamide and immunotherapy could support the translation of these findings into clinical practice and guide treatment decisions. Furthermore, investigating the optimal timing and dosing of evofosfamide in combination with immunotherapy, as well as exploring other hypoxia-targeting strategies, could further optimize the therapeutic outcomes. Understanding the dynamic changes in tumor hypoxia during the course of treatment and tailoring interventions accordingly could lead to enhanced treatment responses and improved patient survival rates.

In conclusion, our study highlights the significance of tumor hypoxia in immunotherapy response and the potential of evofosfamide to modulate hypoxia and improve treatment outcomes. By leveraging FMISO PET imaging and analyzing various hypoxia metrics, we have provided valuable insights into the heterogeneity and severity of hypoxia within tumors. These findings contribute to the development of personalized

cancer treatment approaches and pave the way for future research aiming to overcome the limitations imposed by tumor hypoxia.

REFERENCES

1. Sung, H., et al., *Global cancer statistics 2020: GLOBOCAN estimates of incidence and mortality worldwide for 36 cancers in 185 countries.* CA: a cancer journal for clinicians, 2021. **71**(3): p. 209-249.
2. Organization, W.H., *WHO report on cancer: setting priorities, investing wisely and providing care for all.* 2020.
3. Xi, Y. and P. Xu, *Global colorectal cancer burden in 2020 and projections to 2040.* Translational oncology, 2021. **14**(10): p. 101174.
4. Ahmed, M., *Colon Cancer: A Clinician's Perspective in 2019.* Gastroenterology Res, 2020. **13**(1): p. 1-10.
5. Malki, A., et al., *Molecular Mechanisms of Colon Cancer Progression and Metastasis: Recent Insights and Advancements.* Int J Mol Sci, 2020. **22**(1).
6. Xu, K., et al., *Hypoxia Induces Drug Resistance in Colorectal Cancer through the HIF-1α/miR-338-5p/IL-6 Feedback Loop.* Mol Ther, 2019. **27**(10): p. 1810-1824.
7. Meng, L., et al., *Tumor Oxygenation and Hypoxia Inducible Factor-1 Functional Inhibition via a Reactive Oxygen Species Responsive Nanoplatform for Enhancing Radiation Therapy and Abscopal Effects.* ACS Nano, 2018. **12**(8): p. 8308-8322.
8. Sullivan, R., et al., *Hypoxia-induced resistance to anticancer drugs is associated with decreased senescence and requires hypoxia-inducible factor-1 activity.* Molecular cancer therapeutics, 2008. **7**(7): p. 1961-1973.

9. Nagaraju, G.P., et al., *Hypoxia inducible factor-1α: Its role in colorectal carcinogenesis and metastasis.* Cancer letters, 2015. **366**(1): p. 11-18.

10. Tsiatas, M., G. Mountzios, and G. Curigliano, *Future perspectives in cancer immunotherapy.* Ann Transl Med, 2016. **4**(14): p. 273.

11. Esfahani, K., et al., *A Review of Cancer Immunotherapy: From the Past, to the Present, to the Future.* Current Oncology, 2020. **27**(12): p. 87-97.

12. Nadal, E., et al., *Immunotherapy with checkpoint inhibitors in non-small cell lung cancer: insights from long-term survivors.* Cancer Immunol Immunother, 2019. **68**(3): p. 341-352.

13. Hodi, F.S., et al., *Improved survival with ipilimumab in patients with metastatic melanoma.* New England Journal of Medicine, 2010. **363**(8): p. 711-723.

14. Schadendorf, D., et al., *Pooled Analysis of Long-Term Survival Data From Phase II and Phase III Trials of Ipilimumab in Unresectable or Metastatic Melanoma.* J Clin Oncol, 2015. **33**(17): p. 1889-94.

15. Bai, R., et al., *Mechanisms of Cancer Resistance to Immunotherapy.* Frontiers in Oncology, 2020. **10**.

16. Rieth, J. and S. Subramanian, *Mechanisms of intrinsic tumor resistance to immunotherapy.* International journal of molecular sciences, 2018. **19**(5): p. 1340.

17. Abbott, M. and Y. Ustoyev. *Cancer and the immune system: the history and background of immunotherapy*. in *Seminars in oncology nursing*. 2019. Elsevier.

18. Jenkins, R.W., D.A. Barbie, and K.T. Flaherty, *Mechanisms of resistance to immune checkpoint inhibitors.* British journal of cancer, 2018. **118**(1): p. 9-16.

19. Disis, M.L., *Immune regulation of cancer.* Journal of Clinical Oncology, 2010. **28**(29): p. 4531-4538.

20. Wolf, N.K., D.U. Kissiov, and D.H. Raulet, *Roles of natural killer cells in immunity to cancer, and applications to immunotherapy.* Nature Reviews Immunology, 2023. **23**(2): p. 90-105.

21. Rosenberg, J. and J. Huang, *CD8+ T cells and NK cells: parallel and complementary soldiers of immunotherapy.* Current opinion in chemical engineering, 2018. **19**: p. 9-20.

22. Bagchi, S., R. Yuan, and E.G. Engleman, *Immune checkpoint inhibitors for the treatment of cancer: clinical impact and mechanisms of response and resistance.* Annual Review of Pathology: Mechanisms of Disease, 2021. **16**: p. 223-249.

23. Robert, C., *A decade of immune-checkpoint inhibitors in cancer therapy.* Nature communications, 2020. **11**(1): p. 3801.

24. Li, B., H.L. Chan, and P. Chen, *Immune checkpoint inhibitors: basics and challenges.* Current medicinal chemistry, 2019. **26**(17): p. 3009-3025.

25. Shiravand, Y., et al., *Immune checkpoint inhibitors in cancer therapy.* Current Oncology, 2022. **29**(5): p. 3044-3060.

26. de Coaña, Y.P., A. Choudhury, and R. Kiessling, *Checkpoint blockade for cancer therapy: revitalizing a suppressed immune system.* Trends in molecular medicine, 2015. **21**(8): p. 482-491.

27. Thouvenin, J., et al., *Complete Response in Metastatic Clear Cell Renal Cell Carcinoma Patients Treated with Immune-Checkpoint Inhibitors: Remission or Healing? How to Improve Patients' Outcomes?* Cancers, 2023. **15**(3): p. 793.

28. de Miguel, M. and E. Calvo, *Clinical challenges of immune checkpoint inhibitors.* Cancer cell, 2020. **38**(3): p. 326-333.

29. Kopecka, J., et al., *Hypoxia as a driver of resistance to immunotherapy.* Drug Resistance Updates, 2021: p. 100787.

30. Brahimi-Horn, M.C., J. Chiche, and J. Pouysségur, *Hypoxia and cancer.* Journal of molecular medicine, 2007. **85**: p. 1301-1307.

31. Gruber, M. and M.C. Simon, *Hypoxia-inducible factors, hypoxia, and tumor angiogenesis.* Current opinion in hematology, 2006. **13**(3): p. 169-174.

32. Yang, C., et al., *Analysis of hypoxia-induced metabolic reprogramming.* Methods in enzymology, 2014. **542**: p. 425-455.

33. Abou Khouzam, R., et al., *Tumor hypoxia regulates immune escape/invasion: influence on angiogenesis and potential impact of hypoxic biomarkers on cancer therapies.* Frontiers in Immunology, 2021. **11**: p. 613114.

34. Spiegelberg, L., et al., *Hypoxia-activated prodrugs and (lack of) clinical progress: The need for hypoxia-based biomarker patient selection in phase III clinical trials.* Clinical and translational radiation oncology, 2019. **15**: p. 62-69.

35. Vordermark, D. and M.R. Horsman, *Hypoxia as a biomarker and for personalized radiation oncology.* Molecular Radio-Oncology, 2016: p. 123-142.

36. Mortezaee, K. and J. Majidpoor, *The impact of hypoxia on immune state in cancer.* Life sciences, 2021. **286**: p. 120057.

37. Fu, Z., et al., *Tumour hypoxia-mediated immunosuppression: mechanisms and therapeutic approaches to improve cancer immunotherapy.* Cells, 2021. **10**(5): p. 1006.

38. Dhani, N., et al. *The clinical significance of hypoxia in human cancers*. in *Seminars in nuclear medicine*. 2015. Elsevier.

39. Vikram, D.S., J.L. Zweier, and P. Kuppusamy, *Methods for noninvasive imaging of tissue hypoxia.* Antioxidants & redox signaling, 2007. **9**(10): p. 1745-1756.

40. D'Alonzo, R.A., et al., *In vivo noninvasive preclinical tumor hypoxia imaging methods: a review.* International Journal of Radiation Biology, 2021. **97**(5): p. 593-631.

41. Vito, A., N. El-Sayes, and K. Mossman, *Hypoxia-driven immune escape in the tumor microenvironment.* Cells, 2020. **9**(4): p. 992.

42. C Gaertner, F., et al., *Imaging of hypoxia using PET and MRI.* Current pharmaceutical biotechnology, 2012. **13**(4): p. 552-570.

43. Kircher, M.F., H. Hricak, and S.M. Larson, *Molecular imaging for personalized cancer care.* Molecular oncology, 2012. **6**(2): p. 182-195.

44. Schillaci, O. and N. Urbano, *Digital PET/CT: a new intriguing chance for clinical nuclear medicine and personalized molecular imaging.* European Journal of Nuclear Medicine and Molecular Imaging, 2019. **46**(6): p. 1222-1225.

45. Bar-Shalom, R., et al., *Clinical performance of PET/CT in evaluation of cancer: additional value for diagnostic imaging and patient management.* Journal of nuclear medicine, 2003. **44**(8): p. 1200-1209.

46. Sorace, A.G., et al. *Imaging for response assessment in cancer clinical trials*. in *Seminars in nuclear medicine*. 2020. Elsevier.

47. Beaton, L., et al., *How rapid advances in imaging are defining the future of precision radiation oncology.* British journal of cancer, 2019. **120**(8): p. 779-790.

48. Michael, G., *X-ray computed tomography.* Physics Education, 2001. **36**(6): p. 442.

49. McNeal, K.C., *Created with BioRender.com*.

50. Padhani, A. and L. Ollivier, *The RECIST criteria: implications for diagnostic radiologists.* The British journal of radiology, 2001. **74**(887): p. 983-986.

51. Li, Z. and P.S. Conti, *Radiopharmaceutical chemistry for positron emission tomography.* Advanced drug delivery reviews, 2010. **62**(11): p. 1031-1051.

52. Moses, W.W., *Fundamental limits of spatial resolution in PET.* Nuclear Instruments and Methods in Physics Research Section A: Accelerators, Spectrometers, Detectors and Associated Equipment, 2011. **648**: p. S236-S240.

53. Carter, L.M., et al., *The impact of positron range on PET resolution, evaluated with phantoms and PHITS Monte Carlo simulations for conventional and non-conventional radionuclides.* Molecular imaging and biology, 2020. **22**: p. 73-84.

54. Cegla, P., et al., *Assessment of biological parameters in head and neck cancer based on in vivo distribution of 18F-FDG-FLT-FMISO-PET/CT images.* Tumori Journal, 2020. **106**(1): p. 33-38.

55. Wadsak, W. and M. Mitterhauser, *Basics and principles of radiopharmaceuticals for PET/CT.* European journal of radiology, 2010. **73**(3): p. 461-469.

56. Lau, J., et al., *Insight into the Development of PET Radiopharmaceuticals for Oncology.* Cancers, 2020. **12**(5): p. 1312.

57. Lee, S.T. and A.M. Scott. *Hypoxia positron emission tomography imaging with 18F-fluoromisonidazole*. in *Seminars in nuclear medicine*. 2007. Elsevier.

58. Masaki, Y., et al., *FMISO accumulation in tumor is dependent on glutathione conjugation capacity in addition to hypoxic state.* Annals of Nuclear Medicine, 2017. **31**: p. 596-604.

59. Thorwarth, D., et al., *A kinetic model for dynamic [18F]-Fmiso PET data to analyse tumour hypoxia.* Physics in Medicine & Biology, 2005. **50**(10): p. 2209.

60. Tanguy, J., et al., *[18 F] FMISO PET/CT imaging of hypoxia as a non-invasive biomarker of disease progression and therapy efficacy in a preclinical model of pulmonary fibrosis: comparison with the [18 F] FDG PET/CT approach.* European Journal of Nuclear Medicine and Molecular Imaging, 2021: p. 1-17.

61. Eschmann, S.-M., et al., *Prognostic impact of hypoxia imaging with 18F-misonidazole PET in non-small cell lung cancer and head and neck cancer before radiotherapy.* Journal of nuclear medicine, 2005. **46**(2): p. 253-260.

62. Bruehlmeier, M., et al., *Assessment of hypoxia and perfusion in human brain tumors using PET with 18F-fluoromisonidazole and 15O-H2O.* Journal of Nuclear Medicine, 2004. **45**(11): p. 1851-1859.

63. Kelada, O.J. and D.J. Carlson, *Molecular imaging of tumor hypoxia with positron emission tomography.* Radiation research, 2014. **181**(4): p. 335-349.

64. Reeves, K.M., et al., *18F-FMISO PET imaging identifies hypoxia and immunosuppressive tumor microenvironments and guides targeted evofosfamide therapy in tumors refractory to PD-1 and CTLA-4 inhibition.* Clinical Cancer Research, 2022. **28**(2): p. 327-337.

65. Kroenke, M., et al., *Voxel based comparison and texture analysis of 18F-FDG and 18F-FMISO PET of patients with head-and-neck cancer.* PLoS One, 2019. **14**(2): p. e0213111.

66. Sorace, A.G., et al., *Quantitative [18 F] FMISO PET imaging shows reduction of hypoxia following trastuzumab in a murine model of HER2+ breast cancer.* Molecular imaging and biology, 2017. **19**: p. 130-137.

67. Hunter, F.W., B.G. Wouters, and W.R. Wilson, *Hypoxia-activated prodrugs: paths forward in the era of personalised medicine.* British journal of cancer, 2016. **114**(10): p. 1071-1077.

68. Brender, J.R., et al., *Hypoxia Imaging As a Guide for Hypoxia-Modulated and Hypoxia-Activated Therapy.* Antioxidants & Redox Signaling, 2022. **36**(1-3): p. 144-159.

69. Kishimoto, S., et al., *Hypoxia-activated prodrug evofosfamide treatment in pancreatic ductal adenocarcinoma xenografts alters the tumor redox status to potentiate radiotherapy.* Antioxidants & Redox Signaling, 2021. **35**(11): p. 904-915.

70. Constantinidou, A. and W.T. van der Graaf, *The fate of new fosfamides in phase III studies in advanced soft tissue sarcoma.* European Journal of Cancer, 2017. **84**: p. 257-261.

71. Hegde, A., et al., *A Phase I Dose-Escalation Study to Evaluate the Safety and Tolerability of Evofosfamide in Combination with Ipilimumab in Advanced Solid MalignanciesPhase I Study of Evofosfamide and Ipilimumab in Solid Tumors.* Clinical Cancer Research, 2021. **27**(11): p. 3050-3060.

72. Mudassar, F., et al., *Improving the synergistic combination of programmed death-1/programmed death ligand-1 blockade and radiotherapy by targeting the hypoxic tumour microenvironment.* Journal of Medical Imaging and Radiation Oncology, 2022. **66**(4): p. 560-574.

73. Jing, X., et al., *Role of hypoxia in cancer therapy by regulating the tumor microenvironment.* Molecular cancer, 2019. **18**: p. 1-15.

74. Paredes, F., H.C. Williams, and A. San Martin, *Metabolic adaptation in hypoxia and cancer.* Cancer letters, 2021. **502**: p. 133-142.

75. You, L., et al., *The role of hypoxia-inducible factor 1 in tumor immune evasion.* Medicinal research reviews, 2021. **41**(3): p. 1622-1643.

76. Vallabhajosula, S. *18F-labeled positron emission tomographic radiopharmaceuticals in oncology: an overview of radiochemistry and mechanisms of tumor localization*. in *Seminars in nuclear medicine*. 2007. Elsevier.

77. Lim, J.-L. and M.S. Berridge, *An efficient radiosynthesis of [18F] fluoromisonidazole.* Applied radiation and isotopes, 1993. **44**(8): p. 1085-1091.

78. Patt, M., M. Kuntzsch, and H. Machulla, *Preparation of [18 F] fluoromisonidazole by nucleophilic substitution on THP-protected precursor: yield dependence on reaction parameters.* Journal of radioanalytical and nuclear chemistry, 1999. **240**(3): p. 925-927.

79. Tang, G., et al., *Fully automated one-pot synthesis of [18F] fluoromisonidazole.* Nuclear medicine and biology, 2005. **32**(5): p. 553-558.

80. Liu, Z., et al., *Tumor vasculatures: a new target for cancer immunotherapy.* Trends in pharmacological sciences, 2019. **40**(9): p. 613-623.

81. Azad, A., et al., *PD-L1 blockade enhances response of pancreatic ductal adenocarcinoma to radiotherapy.* EMBO molecular medicine, 2017. **9**(2): p. 167-180.